



## Fouling studies of capillary ultrafiltration membrane

V.S. Mamtani\*, K.P. Bhattacharyya, S. Prabhakar, P.K. Tewari

*Desalination Division, Bhabha Atomic Research Centre, Trombay, Mumbai 400 085, India*

*Tel. +91 22 25594740; email: [vmamtani@barc.gov.in](mailto:vmamtani@barc.gov.in)*

Received 16 April 2012; Accepted 30 September 2013

---

### ABSTRACT

Ultrafiltration (UF) membranes in capillary configuration are deployed in domestic water purification with respect to removal of contaminants. Fouling is an inherent phenomenon in UF process and has been reported to cause decline in flux, reduces membrane life, etc. So, it has to be thoroughly studied in order to optimize the logistics of process operation. Considering the concentration of contaminants in different parts of India, the fouling studies investigations were carried out in the range of 5–15 ppm of various constitutes such as Iron, Manganese, and the organic foulants – sodium alginate and humic acid. Out of various parameters affecting fouling like feed pressure, feed temperature, feed pH, the effort was directed towards studying the effect of various foulants (and at different loadings) on the membrane. Results obtained from experiments suggest that the fouling caused by the organics (sodium alginate and humic acid) is higher than that of inorganics (iron and manganese). Iron caused higher fouling than manganese. Sodium alginate caused higher fouling than humic acid. It is observed that humic acid caused more irreversible fouling than sodium alginate. Attempts have been made to develop a mathematical model to represent the fouling phenomena. The effect of fouling for different loadings of various foulants was seen in terms of change in transmembrane pressure (TMP), under conditions of constant permeate flow. TMP in the proposed model is expressed as the function of feed flow rate, intrinsic membrane porosity, permeability of the membrane, and the plugging constant. The values of plugging constant represent the interactions between the feed and the membrane and thus suggest the degree of fouling, both reversible and irreversible fouling, caused by different foulants and at different loadings. Irreversible pore constriction fraction is a measure of irreversible fouling and it has also been determined for different foulants and at different loadings.

*Keywords:* Ultrafiltration; Fouling; Trans-membrane pressure; Plugging constant; Irreversible pore constriction fraction

---

### 1. Introduction

Ultrafiltration (UF) is a pressure-driven membrane process having wide industrial applications including

water purification. UF membrane in capillary configuration has high packing density, is amenable for easy backwash, causes lower pressure drop, etc. Off late UF-based system was developed and deployed in domestic water purification with respect to removal of

\*Corresponding author. email: [vmamtani@barc.gov.in](mailto:vmamtani@barc.gov.in)

*Presented at the DAE—BRNS Biennial Symposium on Emerging Trends in Separation Science and Technology (SESTEC 2012) Mumbai, India, 27 February–1 March 2012*

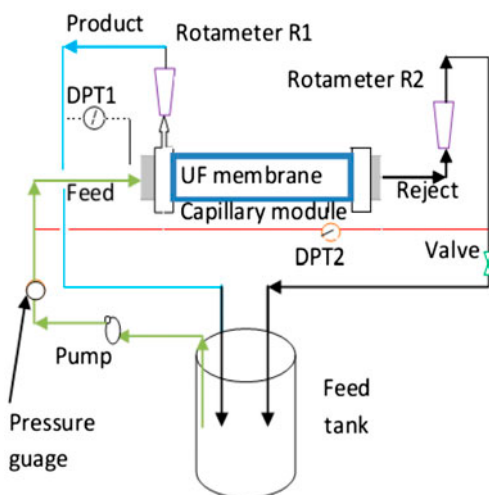


Fig. 1. Schematic of experimental set-up during normal operation.

bio-organism and chemical contaminants such as iron, manganese, sodium alginate, and humic acid [1–3]. Fouling is an inherent phenomenon in UF process and has been reported to cause gradual flux decline, loss of membrane life, and unacceptable product quality apart from increase in energy consumption. So it has to be thoroughly studied in order to optimise the logistics of process operation to ensure sustainability and reliability [4].

Fouling is broadly divided into reversible and irreversible fouling, based on the attachment strength of particles to the membrane surface. Reversible fouling is removable by backwashing while irreversible fouling involves strong attachment of particles which cannot be removed by backwashing. Minimisation of membrane fouling is essential to make membrane processes more effective. Any attempt to minimise fouling requires an understanding of the causes and their relative contribution. A number of fouling studies are reported [4–9] as they are being applied to pretreatment of seawater RO, in applications of effluent treatment and in bioreactor, etc. [4]. Most of them studied fouling in a gross manner without any specific reference to a particular foulant. In domestic water purification for specific contaminants, there is a need to study the fouling characteristics with respect to individual contaminants.

In the present study, the scope of work is limited to the study of fouling in UF membrane with different foulants namely iron (Fe), manganese (Mn), sodium alginate (SA), and humic acid (HA) in the feed and at various loadings, and to do theoretical modeling of the fouling of inside-out capillary UF membrane with cross-flow mode of operation and validating it through

experiments. Theoretical modeling involves prediction of transmembrane pressure (TMP) in a capillary UF membrane for different foulants (Fe, Mn, HA and SA).

## 2. Experimental

### 2.1. Materials

Following chemicals, instruments and membrane modules were used for carrying out experiments.

#### 2.1.1. Chemicals

Ferrous sulfate ( $\text{FeSO}_4 \cdot 7\text{H}_2\text{O}$ ), extra pure AR, in powder form, from—SISCO Research Laboratories Private Limited, Mumbai; manganese chloride ( $\text{MnCl}_2 \cdot 4\text{H}_2\text{O}$ ), from West Cost Laboratories, Mumbai; humic acid, CAS No.: 1,415–93–6, from Sigma Aldrich and Sodium Alginate, CAS No.: 9,005–38–3, from Sigma–Aldrich were used for preparing simulated feed water solution for Fe, Mn, HA, and SA respectively. Service water [pH: 7.5–7.6, total dissolved solids: 73 ppm, iron content: below 1 ppm, total hardness: 66 ppm as  $\text{CaCO}_3$ , total alkalinity: 40.5 ppm as  $\text{CaCO}_3$ ] was used for preparing all simulated solutions.

#### 2.1.2. Membrane module

UF capillary/hollow fiber module of Davey make with 1,400–1,450 fibers having internal diameter = 0.8 mm and outer diameter = 1.3 mm of polysulfone membrane material; 100 KDa molecular weight cut-off and nominal membrane area of 7 m<sup>2</sup> with module having diameter of 90 mm and length of 1,100 mm was used to carry out fouling studies. The module was used in inside-out flow configuration.

#### 2.1.3. Instruments

Pressure gauge (0–7 bar, Mass make) was installed in the feed line to measure the inlet pressure. Differential pressure transmitter (make: Thermax Fuji Electric, range: 0–100 mili bar) were installed to measure feed channel pressure (FCP) drop and the TMP. Rotameters were connected in permeate and the reject lines. To measure Fe and Mn in the permeate, atomic absorption spectroscopy (AAS) was used. For organics, i.e. HA or SA, total organic carbon (TOC) analyser was used to detect their levels in permeate.

### 2.2. Experimental procedure

The experimental setup (Fig. 1) was operated in two modes—normal operation and backwash operation. The experimental study has been performed

in a lab-scale set-up, schematic is shown in Fig. 1. The set-up consists of a *single UF* capillary membrane module of above specifications. Feed of 50 litres is prepared with service water in the feed tank, for different foulants at different ppm. The prepared feed solution is pumped through the capillary UF membrane module with inside-out flow. The feed pressure, the FCP and the TMP are noted under constant permeate flow condition. Reject flow and the permeate flow are also noted. The reject and the permeate stream was recycled back into the feed tank. The observations are noted at different time intervals from time,  $t = 0$  min, i.e. when the experiment is just started. The time interval for which observations were noted are 0, 10, 20, 30, 40, and 45 min. After the above steps (Batch 1), backwashing is done for five minutes which only removes reversible fouling. The next batch is performed after the backwashing. For a given foulant and at a given concentration, three batches were performed and for each foulant, the experiments were performed at three concentrations namely 5, 10, and 15 ppm.

### 2.3. Backwashing operation (out to in)

During backwashing operation, the feed line (feed hose) is interchanged with the permeate line (Fig. 2). The backwash is provided to remove reversible fouling. The remaining set-up is same as during normal operating condition.

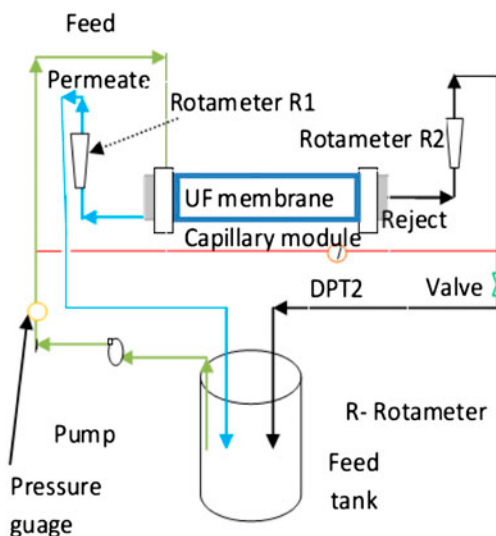


Fig. 2. Schematic of experimental set-up during backwashing.

### 2.4. Chemical cleaning

Chemical cleaning is done so as to remove both reversible and irreversible fouling. It is done before changing the feed condition that is either change of foulant in feed or change of concentration (ppm) of the foulant in feed. It is done so as to restore the porosity of the membrane to the initial value. Feed with diluted HCl having pH around 5 is used for chemical cleaning for inorganic foulant and feed with NaOH having pH around 10 is used for chemical cleaning of organic foulant.

## 3. Results and discussion

The observations found from the experiments were used to obtain graphs which were analyzed to understand the fouling phenomena for different foulants.

### 3.1. TMP vs. time for various foulants at 10 ppm level

The graphs (Figs. 3–6) were plotted for the observed TMP vs. time for 10 ppm of various foulants

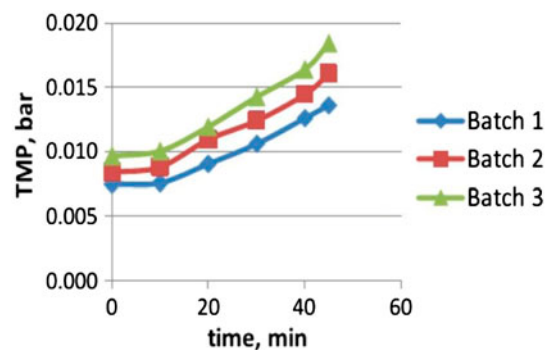


Fig. 3. Variation in TMP with time for 10 ppm Mn as foulant in feed.

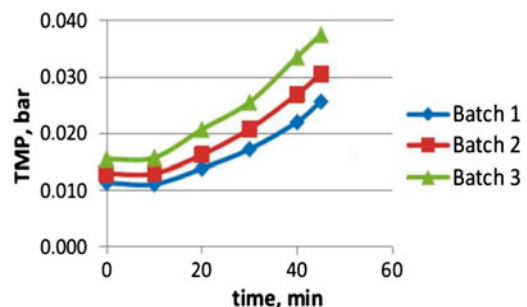


Fig. 4. Variation in TMP with time for 10 ppm Fe as foulant in feed.

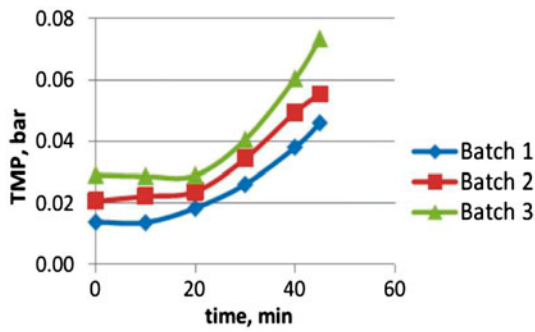


Fig. 5. Variation in TMP with time for 10 ppm humic acid as foulant in feed.

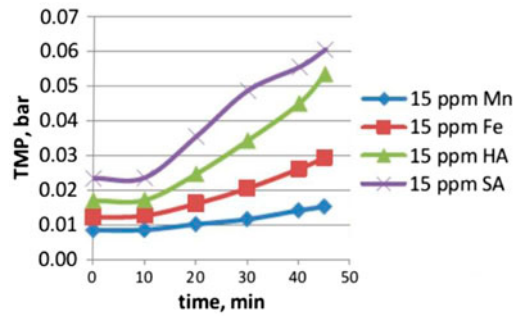


Fig. 8. Variation in TMP with time for different foulants at 15 ppm.

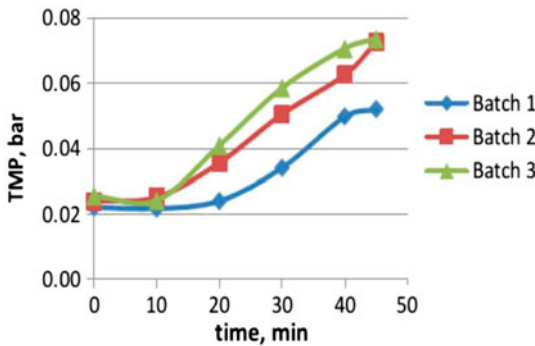


Fig. 6. Variation in TMP with time for 10 ppm Sodium Alginate as foulant in feed.

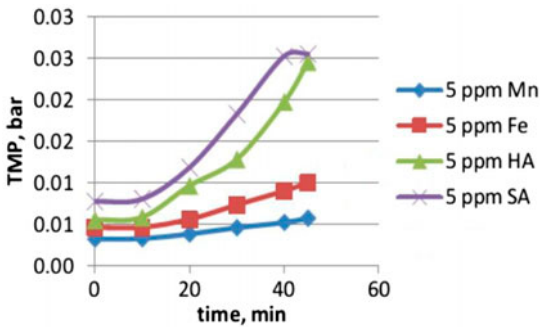


Fig. 7. Variation in TMP with time for different foulants at 5 ppm.

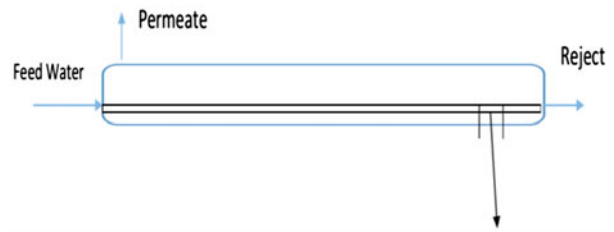


Fig. 9(a). Schematic showing a fiber within a capillary module.

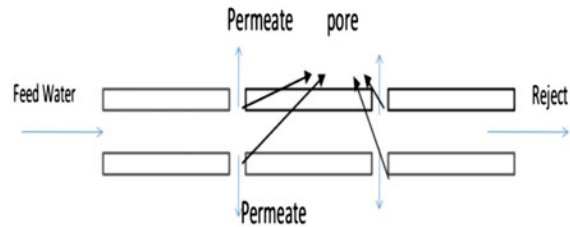


Fig. 9(b). Schematic of a capillary fiber with pores in it, at 0 min (regular cylindrical pores considered).

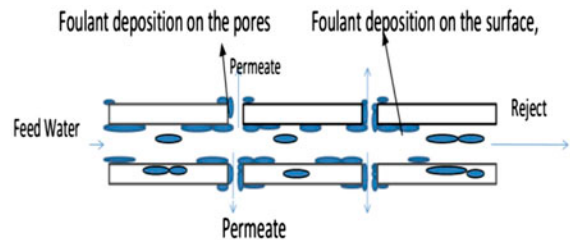


Fig. 9(c). Schematic of a capillary fiber with deposition of foulants on the surface and the pores, at t min (typical).

and for all the three batches of experiments conducted with them.

From the above graphs, it can be observed that the TMP increases with time for each foulant. This is because of the foulant getting deposited on the pores and on the surface of the membrane increasing the resistance for flow through the membrane. We can also see that the TMP in the subsequent batches is

higher. This can be attributed to irreversible fouling caused by the foulant, which cannot be removed by backwashing. It can also be seen from the graphs that

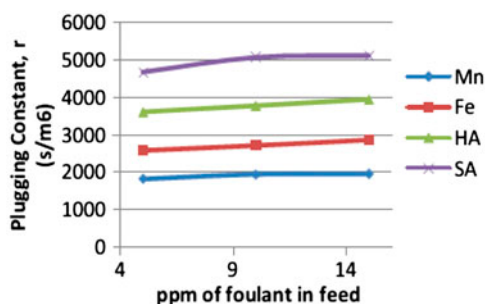
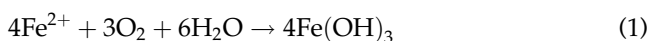


Fig. 10. Variation in plugging constant with ppm of foulant in feed.

the “TMP” and the “increase in TMP with time” for 10 ppm of different foulants is in ascending order of Mn, Fe, HA, and SA respectively. SA and HA are organic foulants and get easily adsorbed on membrane surface. Hence, organic fouling causes more rise in TMP than particle/colloidal fouling caused by inorganic foulant like Fe and Mn, which is most likely to foul the membranes through mechanisms of deposition in pore. However, it should be noted that the inorganic foulant also causes irreversible fouling to a certain extent.

Fouling caused by Fe is more than Mn which is explained as follows. Fe and Mn are in divalent form ( $\text{Fe}^{2+}$ ) and ( $\text{Mn}^{2+}$ ) when the feed is just prepared. The feed was exposed to air and kept overnight which caused  $\text{Fe}^{2+}$ ,  $\text{Mn}^{2+}$  to oxidize into  $\text{Fe}^{3+}$  and  $\text{Mn}^{3+}$  respectively, which form insoluble colloidal hydroxides as shown in the following equations:



The oxidation kinetic rate for Fe is greater than Mn and also oxidation of Fe occurs at a much lower pH than Mn. Hence, colloids formation of Fe is faster and more than Mn. Thus, Fe causes more fouling than Mn, and hence TMP with time for Fe is more than Mn.

Fouling due to SA solution is more than HA which is in line with the common assessment in the literature [1,2,10,11]. This can be attributed to higher molecular weight (of the order  $10^5$  Da) of sodium alginate causing it to form the cake layer on the membrane pores and thus blocking the pores completely, however, it is easily removable by backwashing [12]. SA fouls more severely; initially by rapid irreversible fouling due to internal pore adsorption, causing pore constriction, followed by rapid cake development on the membrane

surface, which later becomes the dominant fouling mechanism i.e. the cake forming on the membrane surface and it can be characterized as a labile layer which is easily removable. HA, on the other hand, causes relatively rapid irreversible fouling due to internal pore adsorption, which persists for a long time. However, reversible pore blocking takes place much slower as compared to SA. Thus, it is observed that even though HA which causes more irreversible fouling; it is SA that fouls more, mainly because of reversible fouling, which can be removed by backwashing. We will see later from the graphs (Figs. 11–13) that irreversible fouling by HA is more as compared to SA. HA, having comparatively lower molecular weight (of the order  $10^4$  Da), causes less deposition on membrane pores but attaches itself irreversibly on the membrane surface, and is not removable by backwashing. The difference in behavior of these organic substances can also be attributed to several other factors, such as different intermolecular adhesion forces developing in the concentrated layer near the membrane surface, different molecular weight distribution and different aggregation tendency.

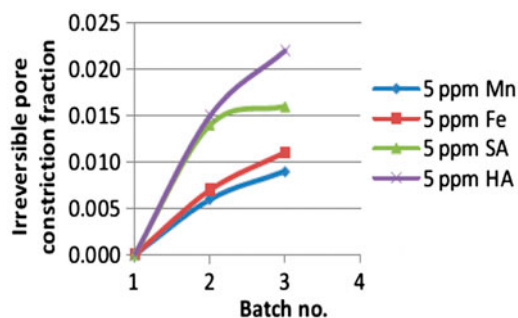


Fig. 11. Variation in irreversible pore constriction with batch no. for different foulants at 5 ppm.

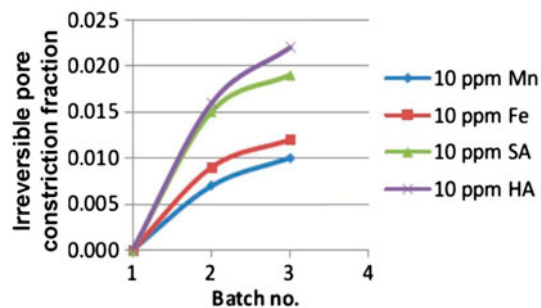


Fig. 12. Variation in irreversible pore constriction with batch no. for different foulants at 10 ppm.

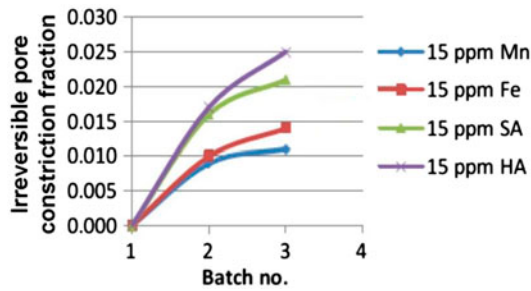


Fig. 13. Variation in irreversible pore constriction with batch no. for different foulants.

### 3.2. TMP vs. Time for different foulants at various loadings

It can be clearly seen from the graphs (Fig. 7 and 8) given above that for all the four foulants at concentration of 5 and 15 ppm for Batch 1, the “TMP” and the “increase in the TMP” is in increasing order of Mn, Fe, HA, and SA which is in agreement with the discussion (3.1). Variation in TMP with time for different foulants at 10 ppm is given in Figs. 3–6.

## 4. Physical phenomena and mathematical modeling

A mathematical model was proposed to predict the TMP based on the physical phenomena taking place.

### 4.1. Physical phenomena

A single cylindrical capillary fiber is shown in Fig. 9(b) which is taken from capillary UF membrane module (Fig. 9(a)). Fig. 9(c) shows the foulant deposition on the pores and at the surface within a single capillary fiber, causing narrowing of the passage for flow across the membrane. The symmetry of the pores is used for simplification. It has been reported that pores appeared to be more preferable sites for adsorption, especially for organic foulant [10]. This may be attributed to higher convective flow through the membrane.

### 4.2. Mathematical modeling of fouling of UF membrane

The mathematical model for describing the fouling of inside-out hollow fiber UF membrane is derived from the hydrodynamic equations coupled with the theory of depth filtration. In which the effects of membrane characterisation, amount of foulant content in feed water, feed water characteristics, and the interactions of foulants with the UF membranes are

expressed with only one parameter defined as membrane plugging coefficient. Membrane filtration tests are conducted with prepared sample water containing the foulants with constant flow (permeate) mode of operation. The correlations obtained in the present study are simpler than those obtained in the previous works [4–8].

Following assumptions were made for developing the mathematical model:

- (1) Steady state, laminar, fully developed, incompressible and Newtonian flow.
- (2) Foulants in the membrane are distributed uniformly and fouling is taking place continuously.
- (3) Membrane pores are uniform in size.
- (4) The change in cross-sectional area to flow is negligible.
- (5) The change in capillary fiber diameter due to fouling is negligible.
- (6) The volume of the accumulated foulant deposited per unit time will be proportional to the TMP at specific position.

$$\frac{d\sigma}{dt} \propto \Delta P \quad (3)$$

where

$$\sigma = \frac{\text{Volume of accumulated fouling particles}}{\text{Volume of membrane}}$$

- (7) The volume of the accumulated foulant deposited per unit time will be proportional to the local flux at the specific position.

$$\frac{d\sigma}{dt} \propto \frac{q}{A} \quad (4)$$

Also,

$$u = \frac{q}{\varepsilon A} = \frac{v_0}{\varepsilon} \quad (5)$$

- (8) The volume of the accumulated foulant deposited per unit time will be proportional to the number of retained particles which is same as the membrane effective porosity ( $\varepsilon$ ).

$$\frac{d\sigma}{dt} \propto \left(1 - \frac{\sigma}{\varepsilon_0}\right) \quad (6)$$

Now,  $\varepsilon = \frac{\text{Pore volume at any instance}}{\text{Volume of membrane}}$

$$\text{And } \varepsilon_0 = \frac{\text{Pore volume at } t = 0}{\text{Volume of membrane}}$$

$$\text{Implies, } \sigma = \varepsilon_0 - \varepsilon \quad (7)$$

Therefore,  $\sigma = 0$  when  $\varepsilon = \varepsilon_0$ ; and  $\sigma = \varepsilon_0$  when  $\varepsilon = 0$ .

#### 4.2.1. Darcy's law

Darcy's Law is a phenomenological derived constitutive equation that describes the flow of a fluid through a porous medium. It is a simple proportional relationship between the instantaneous discharge rate through a porous medium, the viscosity of the fluid and the pressure drop over a given distance.

$$q = \frac{k'A\Delta P}{\mu L} \quad (8)$$

$$\Rightarrow q\alpha\Delta P \quad (9)$$

$$\Rightarrow q = k(\Delta P) \quad (9)$$

$$\Rightarrow q = k\Delta P \quad (10)$$

Combining Eqs. (3), (4), (6), (8), (9); we get

$$\frac{d\sigma}{dt} = r'' \frac{q^2}{A^2} \left(1 - \frac{\sigma}{\varepsilon_0}\right) \quad (11)$$

where  $r''$  is a constant and named as membrane plugging coefficient ( $\text{s}/\text{m}^2$ ) which is determined by membrane characterization, feed water, cleaning methods, etc. As it is assumed that the change in membrane cross-sectional area for flow  $A$  is negligible and thus remains constant. Also, plugging coefficient is constant for a given feed condition and a given membrane; hence,  $r''/A^2$  remains constant for our system and is termed as plugging constant denoted by  $r$ .

Hence, the Eq. (10) becomes,

$$\frac{d\sigma}{dt} = rq^2 \left(1 - \frac{\sigma}{\varepsilon_0}\right) \quad (12)$$

#### 4.2.2. Permeability coefficient $k$ and theory of depth filtration

The permeability coefficient  $k$  is equal to  $k_0$  at the initial filtration stage. However, the permeate flux and the permeability constant will change with the

accumulation of the foulants. The main separation mechanism in UF process is size exclusion. So, the traditional theory of filtration can be used to obtain the relationship between the trans-membrane pressure ( $\Delta P$ ) with the porosity  $\varepsilon$ . The Kozeny–Carman relation, for laminar flow through filtrate is given by Eq. (13).

$$\frac{\Delta P}{L} = \frac{k_1\mu(1-\varepsilon)^2 S^2}{\varepsilon^3} v_0 \quad (13)$$

From Eq. (5)

$$\frac{\Delta P}{L} = \frac{k_1\mu(1-\varepsilon)^2 S^2 q}{\varepsilon^3 A} \quad (14)$$

$$\Rightarrow \Delta P\alpha \frac{(1-\varepsilon)^2}{\varepsilon^3} q \quad (15)$$

Compared with Eq. (10)

$$\Rightarrow k\alpha \frac{\varepsilon^3}{(1-\varepsilon)^2} \quad (16)$$

Now,  $\sigma = \varepsilon_0 - \varepsilon$  or  $\varepsilon = \varepsilon_0 - \sigma$

$$\frac{k}{k_0} = \frac{\varepsilon^3(1-\varepsilon_0)^2}{(1-\varepsilon)^2\varepsilon_0^3} = \frac{(\varepsilon_0 - \sigma)^3(1-\varepsilon_0)^2}{(1-\varepsilon_0 + \sigma)^2\varepsilon_0^3}$$

$$\frac{k}{k_0} = \frac{(1-\sigma/\varepsilon_0)^3}{[1+\sigma/(1-\varepsilon_0)]^2} \quad (17)$$

#### 4.2.3. Establishment of membrane fouling model

A mathematical model for describing the fouling of inside-out capillary UF membrane was derived from the hydrodynamic equations coupled with the theory of depth filtration.

The expression [Eq. (12)] of  $\sigma$  is integrated over the operation time ( $0 \leq t \leq t$ ),

$$\int \left(\frac{\varepsilon_0}{\varepsilon_0 - \sigma}\right) d\sigma = \int_0^t rq^2 dt \quad (18)$$

$$-\varepsilon_0 \ln(\varepsilon_0 - \sigma) = rq^2 t + c \quad (19)$$

At  $t = 0$ ,  $\sigma = \varepsilon_0 - \varepsilon = \varepsilon_0 - \varepsilon_0 = 0$

$\Rightarrow c = -\varepsilon_0 \ln \varepsilon_0$

Substituting  $c$ ,

$$\varepsilon_0 \ln \varepsilon_0 - \varepsilon_0 \ln(\varepsilon_0 - \sigma) = rq^2t \tag{20}$$

$$\varepsilon_0 \ln\left(\frac{\varepsilon_0}{\varepsilon_0 - \sigma}\right) = rq^2t \tag{21}$$

$$\ln\left(\frac{\varepsilon_0 - \sigma}{\varepsilon_0}\right) = -\frac{rq^2t}{\varepsilon_0} \tag{22}$$

$$\sigma = \varepsilon_0 - \varepsilon_0 \exp\left(\frac{-rq^2t}{\varepsilon_0}\right) \tag{23}$$

Since,  $k_0$  can be obtained by Eq. (10) according to initial TMP and permeate flow rate. Therefore,  $k$  can be obtained by substitution of Eq. (23) into Eq. (17). The  $k$  value can be used to find the TMP at any time using Eq. (10).

### 4.3. Prediction of TMP with time

#### 4.3.1. Plugging constant

The mathematical model described above is used for calculating the  $r$  (plugging constant) value. The procedure is as mentioned below. Substituting Eq. (23) in Eq. (17),

$$\frac{k}{k_0} = \frac{\left[1 - \frac{\varepsilon_0}{\varepsilon_0} + \frac{\varepsilon_0 \exp\left(\frac{-rq^2t}{\varepsilon_0}\right)}{\varepsilon_0}\right]^3}{\left[1 + \frac{\varepsilon_0}{(1-\varepsilon_0)} - \frac{\varepsilon_0 \exp\left(\frac{-rq^2t}{\varepsilon_0}\right)}{(1-\varepsilon_0)}\right]^2} \tag{24}$$

$$(1 - \varepsilon_0)^2 \frac{k}{k_0} = \frac{\left(\exp\left(\frac{-rq^2t}{\varepsilon_0}\right)\right)^3}{\left[\left(1 - \varepsilon_0 \exp\left(\frac{-rq^2t}{\varepsilon_0}\right)\right)\right]^2} \tag{25}$$

$$\text{Let } G = \exp\left(\frac{-rq^2t}{\varepsilon_0}\right) \tag{26}$$

$$\text{and let } C = (1 - \varepsilon_0)^2 \frac{k}{k_0} \tag{27}$$

Combining Eqs. (25)-(27),

$$C = \frac{G^3}{(1 - \varepsilon_0 G)^3} \tag{28}$$

The value of  $C$  can be calculated as  $k$  and  $k_0$  can be found out using Eq. (10) (with TMP and permeate flow rate being observed data), while  $\varepsilon_0$  is known for a given membrane. Hence, value of  $G$  can be obtained

Table 1

Plugging constant for different foulants at different feed concentration

Foulant (ppm)	Plugging constant $r$ (s/m <sup>6</sup> )			
	Foulant in feed			
	Mn	Fe	HA	SA
5	1,830	2,596	3,607	4,676
10	1,953	2,721	3,777	5,071
15	1,957	2,878	3,950	5,115

from the above Eq. (28) with  $C$  known from Eq. (27). Thus, value of  $r$  can be obtained at different time  $t$  for a given set of observation. The mean value of  $r$  thus obtained will be used for calculation of TMP for new sets of experiments. In this study,  $r$  value is obtained using the observation from first batch.

Plugging constant represents the magnitude of the fouling taking place in the membrane. It represents both reversible and irreversible fouling taking place. It is also known that plugging constant depends on the feed condition; hence, it varies for different foulant and also for different concentration of a given foulant. It can be seen from the graph (Fig. 10) that plugging constant increases with the increase in foulant concentration in the feed, which implies that the plugging or constriction of pores of membrane or the fouling of the membrane increases with the increase in the foulant concentration. It can also be seen that the organic foulant have higher plugging constant as compared to inorganic foulant and that SA causes highest fouling and Mn causes the least fouling among the all the foulants. Table 1 gives the value of plugging constant  $r$  for different feed condition.

#### 4.3.2. Prediction of TMP

The mean value of  $r$  thus obtained is substituted in Eq. (25) to calculate the value of  $k$  at a given time. The  $k$  value thus obtained is used to calculate TMP value at that instant of time using Eq. (10).

#### 4.3.3. Porosity and fraction of irreversible pore constriction

The porosity of the membrane  $\varepsilon_0$  for the first batch is known. The porosity value, however changes after a given batch because of deposition of the foulants in the pores i.e.  $\varepsilon_0$  value after Batch 1 changes.

As backwashing is done after a given batch which removes only reversible fouling, while irreversible

fouling is not removed. Therefore, the  $r$  value obtained from the first batch is used and the first observation (TMP value at  $t = 10$  min, of the batch for which  $\varepsilon_0$  is to be found out) is used to calculate the  $\varepsilon_0$  value of the new batch. The difference in  $\varepsilon_0$  value of the two batch gives irreversible pore constriction i.e. fraction of pore constricted irreversibly or fraction of pore constricted due to irreversibly fouling.

Irreversible pore constriction fraction was found at different batches for a given concentration of a foulant. It can be seen from Fig. 11–13 that irreversible constriction of pore is highest in HA. SA also causes high irreversible constriction of pore initially but later tends to be less as compared to the HA. It can also be seen that Fe and Mn also constrict the pore irreversibly to a lesser extent.

For all the foulants, it can be seen that the irreversible constriction of pore increases as the operation period (batch) increases but it approaches to constant value suggesting saturation of the adsorption (organics)/precipitation (inorganics) of the foulants inside the membrane pores.

#### 4.3.4. Experimental validation of mathematical model

The proposed mathematical model as described earlier was used to predict TMP value for the 2nd and 3rd batch for different foulants at 10 ppm concentration. The observed value of TMP and predicted value obtained using the model were plotted with respect to time so as to compare them. The various graphs obtained as shown below (Figs. 14–17) indicate that the proposed model quite accurately predicts the TMP with respect to time, and thus validating the proposed model. It may be noted that, in case of sodium alginate, the fouling is mainly reversible in nature. The application of high TMP may have caused forward flushing that removes the foulant, and thus nullifying

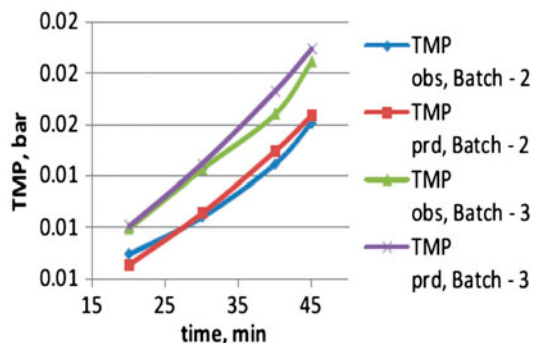


Fig. 14. Variation in TMP observed and TMP predicted with time; 10 ppm manganese in feed.

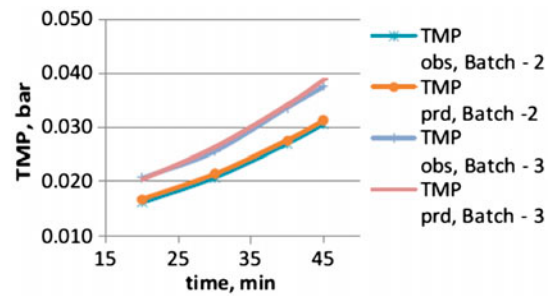


Fig. 15. Variation in TMP observed and TMP predicted with time; 10 ppm iron in feed.

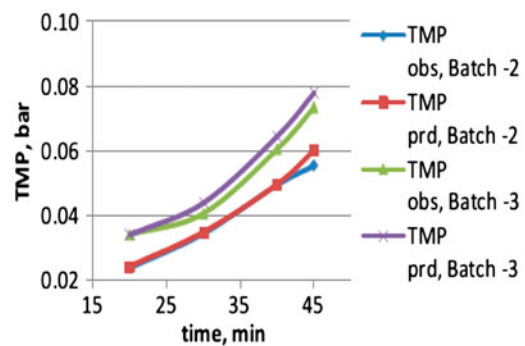


Fig. 16. Variation in TMP observed and TMP predicted with time; 10 ppm humic acid in feed.

the requirement of higher TMP for maintaining same permeate flow rate. The proposed model has limitation in assumption that fouling should take place continuously in the membrane. So, some variation (around 18% of TMP) in between predicted TMP and actual TMP values can be seen at higher TMP value ( $y$ -axis) in Fig. 17.

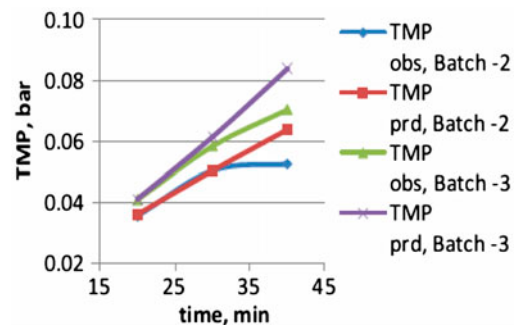


Fig. 17. Variation in TMP observed and TMP predicted with time; 10 ppm sodium alginate in feed.

## 5. Conclusion

Following points are concluded after carrying out the experimental studies.

- Fouling caused by organic foulant is more compared to the inorganic foulant.
- Fouling caused by Fe is more as compared to Mn. Inorganic foulant mainly causes reversible fouling but also causes to certain extent irreversible fouling.
- Fouling caused by SA is more compared to HA. However, irreversible fouling caused by HA is more than that due to SA.
- The proposed model can *satisfactorily* explain the fouling process.

## Acknowledgments

We are thankful to Dr A.K. Ghosh and Smt. Payel Sarkar of Desalination Division, B.A.R.C for their guidance on technical aspects of the experiment.

## Nomenclature

$A$	— membrane cross-sectional area for flow; $m^2$
$C/G$	— constants
$k$	— permeability coefficient; $m^5/N.s$
$k'$	— permeability of membrane; Darcy
$k_1$	— constant depending on particle (foulant) size and shape
$L$	— length of the porous channel across the membrane; m
$\Delta P$	— trans-membrane pressure drop; $N/m^2$
$q$	— permeate flow rate, $m^3/s$
$r$	— plugging constant; $s/m^6$
$r''$	— membrane plugging coefficient; $s/m^2$
$S$	— specific surface area of the particle, i.e. area of particle per unit volume of particle; $m^{-1}$
$t$	— time, s
$u$	— permeate velocity; m/s
$v_0$	— superficial velocity; m/s

## Greek

$\varepsilon$	— porosity of the membrane (pore volume/total volume)
$\varepsilon_0$	— porosity of the membrane (pore volume/total volume) at time $t = 0$

$\sigma$	— volume of the accumulated foulant deposited; $m^3$
$\mu$	— viscosity of the fluid flowing through the membrane; $N.s/m^2$

## References

- [1] K. Katsoufidou, S.G. Yiantsios, A.J. Karabelas, Experimental study of ultrafiltration membrane fouling by sodium alginate and flux recovery by backwashing, *J. Membr. Sci.* 300 (2007) 137–146.
- [2] K. Katsoufidou, S.G. Yiantsios, A.J. Karabelas, An experimental study of UF membrane fouling by humic acid and sodium alginate solutions: The effect of backwashing on flux recovery, *Desalination* 220 (2008) 214–227.
- [3] K.-H. Choo, H. Lee, S.-J. Choi, Iron and manganese removal and membrane fouling during UF in conjunction with prechlorination for drinking water treatment, *J. Membr. Sci.* 267 (2005) 18–26.
- [4] M. Cheryan, *Ultrafiltration Handbook*, Technomic, Dordrecht, 1986.
- [5] G. Bolton, D. LaCasse, R. Kuriyel, Combined models of membrane fouling: Development and application to microfiltration and ultrafiltration of biological fluids, *J. Membr. Sci.* 277 (2006) 75–84.
- [6] J. Marriott, E.S. Hrensen, A general approach to modelling membrane modules, *Chem. Eng. Sci.* 58 (2003) 4975–4990.
- [7] M.F.A. Goosen, S.S. Sablani, H. Al-Hinai, S. Al-Obeidani, R. Al-Belushi, D. Jackson, Fouling of reverse osmosis and ultrafiltration membranes: A critical review, *Sep. Sci. Technol.* 39(10) (2004) 2261–2298.
- [8] P. Bacchin, P. Aimar, V. Sanchez, Model for colloidal fouling of membranes', *AIChE J.* 42(2) (1995) 368–376.
- [9] Y. Li, W. Zhang, X. Zhang, C. Chen, J. Wang, Characterization of fouling in immersed polyvinylidene fluoride hollow fibre membrane ultrafiltration by particles and natural organic matter, *Desalin. Water Treat.* 18 (2010) 309–314.
- [10] M.M. Clark, C. Jucker, Interactions between hydrophobic ultrafiltration membranes and humic substances In *Proc. Membrane Technology Conference*, Baltimore, MD, 1993.
- [11] K. Katsoufidou, S.G. Yiantsios, A.J. Karabelas, Experimental study of ultrafiltration membrane fouling by sodium alginate and flux recovery by backwashing, *J. Membr. Sci.* 300 (2007) 137–146.
- [12] M.D. Kennedy, J. Kamany, B.G.J. Heijman, G. Amy, Colloidal organic matter fouling of UF membranes: Role of NOM composition and size, *Desalination* 220 (2008) 200–213.